The human eye is an example of robust optical design

Pablo Artal Laboratorio de Optica, Departamento de Física, Universidad de Murcia, Campus de Espinardo, Murcia, Spain

Antonio Benito Laboratorio de Optica, Departamento de Física, Universidad de Murcia, Campus de Espinardo, Murcia, Spain

Juan Tabernero Laboratorio de Optica, Departamento de Física, Universidad de Murcia, Campus de Espinardo, Murcia, Spain

In most eyes, in the fovea and at best focus, the resolution capabilities of the eye's optics and the retinal mosaic are remarkably well adapted. Although there is a large individual variability, the average magnitude of the high order aberrations is similar in groups of eyes with different refractive errors. This is surprising because these eyes are comparatively different in shape: Myopic eyes are longer whereas hyperopic eyes are shorter. In most young eyes, the amount of aberrations for the isolated cornea is larger than for the complete eye, indicating that the internal ocular optics (mainly the crystalline lens) play a significant role in compensating for the corneal aberrations, thereby producing an improved retinal image. In this paper, we show that this compensation is larger in the less optically centered eyes that mostly correspond to hyperopic eyes. This suggests a type of mechanism in the eye's design that is the most likely responsible for this compensation. Spherical aberration of the cornea is partially compensated by that of the lens in most eyes. Lateral coma is also compensated mainly in hyperopic eyes. We found that the distribution of aberrations between the cornea and lens appears to allow the optical properties of the eye to be relatively insensitive to variations arising from eye growth or exact centration and alignment of the eye's optics relative to the fovea. These results may suggest the presence of an auto-compensation mechanism that renders the eye's optics robust despite large variation in the ocular shape and geometry.

Keywords: optical aberrations, human eye, refraction, auto-calibration mechanism

Introduction

The human eye, like any optical instrument, is affected by aberrations that degrade the retinal image and ultimately limit spatial vision. Each individual has a distinct aberration pattern (Artal & Navarro, 1994; Howland & Howland, 1976; Liang and Williams, 1997), and the overall amount can vary from eye to eye in normal eyes. However, in a population, the average magnitude of aberrations in a group of emmetropic eyes is similar to that found in groups of mild to moderate myopes and hyperopes (Cheng, Bradley, Hong, & Thibos, 2003). This is intriguing because the size and shape of the eye is very dependent on the refractive state: Myopic eyes having characteristically longer axial lengths than hyperopic ones (Grosvenor & Goss, 1999). How the relatively simple, from an optical point of view, ocular components, the cornea and crystalline lens, are formed to produce a similar optical resolution in average at best focus, independently of the large structural ocular differences, is not well understood. In recent years, the use of advanced optical technology (Fernández, Iglesias, & Artal, 2001; Hofer, Artal, Singer, Aragón, & Williams, 2001) allowed researchers to study the relative contribution of the ocular optical elements (Artal & Guirao, 1998; Artal, Guirao, Berrio, & Williams, 2001; Kelly, Mihashi, & Howland, 2004). In most young eyes, the magnitude of aberrations for both the cornea and the lens are larger than for the complete eye, indicating a significant role of the lens in compensating for the corneal aberrations and thus producing improved retinal images. However, in older subjects the opposite situation occurs: The lens adds aberrations to the cornea yielding a complete system with poorer optical quality (Artal, Berrio, Guirao, & Piers, 2002). The changes in the shape and size of the lens through life (Glasser & Campbell, 1998) may explain the progressive lack of compensation occurring in older eyes.

Either active or passive adaptive mechanisms could be responsible for the aberration compensation in young eyes (Kelly et al., 2004). We refer as active adaptation that occurring during the individual life span and passive that determined genetically through evolution. An active mechanism, for instance, the precise modification of lenticular aberration to cancel those of the cornea, would require a complicated process, even more sophisticated than the one possibly involved in compensating defocus in the emmetropization process occurring during development (Schaeffel & Diether, 1999). A passive mechanism would simply be determined by the average aberrations present in both the cornea and the lens due to the evolutionary process. An optimized eye's design should be robust enough

doi: 10.1167/6.1.1 Received July 26, 2005; published January 10, 2006 ISSN 1534-7362

to provide acceptable quality for different geometry of eyes. If that is the case, aberration compensation may depend on the particular eye geometry, generally dependent on the refractive error. In this context, we carried out an experiment to measure the optical properties of eyes in subjects with different refractive states.

Methods

We measured the optical properties of eyes in two groups of subjects (myopes and hyperopes) covering a large range of refractive states: from −9 to +8 D. In each eye, the wave aberration of the complete eye, considered as one single imaging system, was measured by using a Hartmann–Shack wavefront sensor (Liang, Grimm, Goelz, & Bille, 1994). This system, described elsewhere (Prieto, Vargas-Martín, Goelz, & Artal, 2000), consists of a microlens array, conjugated with the eye's pupil, and a camera placed at its focal plane. If a plane wavefront reaches the microlenses array, the camera records a perfectly regular mosaic of spots. However, if a distorted (i.e., aberrated) wavefront reaches the sensor, the pattern of spots is irregular. The displacement of each spot is proportional to the derivative of the wavefront over each microlens area. From the images of the spots, the ocular wave aberration is computed and expressed as a Zernike polynomial expansion (Noll, 1976). The wave aberration of the cornea was computed from elevation data obtained by a corneal topographer by performing a ray tracing through the corneal surface. Corneal elevations at a sample of points were obtained with a Placido-based corneal topographer (Atlas, Carl Zeiss-Meditec, Dublin, CA, USA). From the corneal elevations, an analytical expression for the corneal surface was obtained by fitting the sample data to a Zernike polynomial representation and then fitted to a bi-cubic spline function. An optical design software package (ZEMAX Development Corp, San Diego, CA) was used to perform ray tracing through this surface and calculate the aberrations associated to the corneal surface. This is a slightly modified procedure providing similar results as that previously described (Guirao & Artal, 2000).

The wavefront aberration of the crystalline lens was estimated by direct subtraction of the corneal from the ocular aberrations. By using an effective index of refraction for the cornea, we partially include the contribution of the posterior corneal surface within the corneal aberrations (Guirao & Artal, 2000). Figure 1 shows a schematic representation of the procedure. In a simple model, having the two series of Zernike coefficients, both for the cornea (c_{nm}) and the eye (c_{nm}''), the aberrations of the lens are obtained by direct subtraction of each pair of coefficients (c_{nm}').

It is assumed that the changes in the wave aberration are small for different axial planes; that is, from the corneal vertex to the pupil plane. To have a correct reference for registration, the ocular and corneal aberration maps were realigned to the geometrical center of the pupil. A detailed discussion on the problems of combining corneal and ocular aberrations is described elsewhere (Artal, 2004).

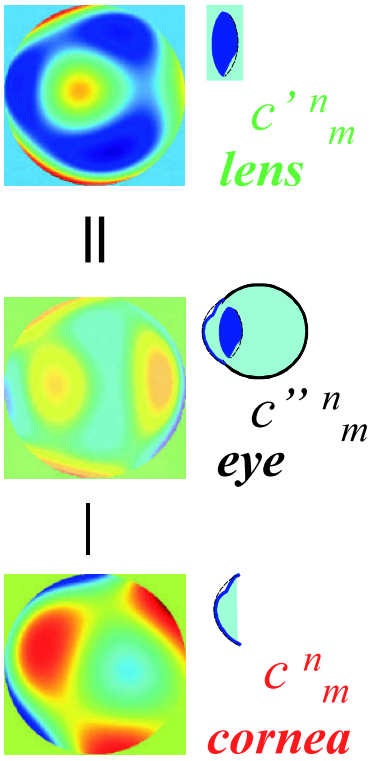

Figure 1. Schematic diagram of the procedure to estimate the aberrations of the lens from corneal and ocular measurements.

All the aberration analyses were completed for 6-mm pupil diameter. In every eye, the location of the pupil center with respect to the corneal apex is determined from the corneal topography data. The distance from the pupil center to the corneal apex (X, Y) provides information on the eye's geometry and is directly related to angle kappa (κ), which is formed between the pupillary axis and the visual axis. The pupillary axis is the line from the center of the entrance pupil that intersects perpendicularly the cornea and the visual axis is the line that connects the fixation point and the fovea in the retina through the eye's nodal points (Le Grand & El Hage, 1980). Figure 2 shows schematically this situation. In shorter eyes with larger angle kappa the displacement of the corneal reflex (X) is usually also larger.

The complete set of measurements was performed in 73 eyes: 57 myopes with an average age of 29.7 years old (*SD* 7.1 years) and 16 hyperopes with and average age of 33 years old (*SD* 7.9 years). Both right (36) and left (37) eyes were measured. The study followed the tenets of the Declaration of Helsinki, and signed informed consent was obtained from every subject after the nature

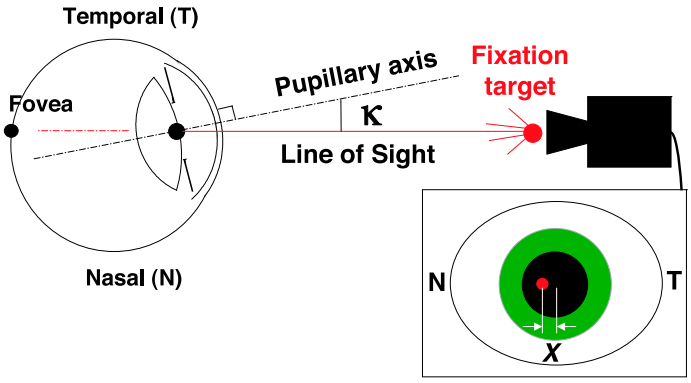

Figure 2. Schematic diagram showing how the kappa angle (κ) is related with the measured displacement of the corneal reflex with respect to the center of the entrance pupil (X).

and all possible consequences of the study had been explained.

Results

Figure 3 shows the magnitude of the aberrations, expressed as the root mean square (RMS) in microns, for the myopic (left) and hyperopic eyes (right). The average amount of aberrations in the complete eye (black circles) was found to be quite similar in both groups of eyes. However, the aberrations of the cornea (red triangles) and lens (green squares) were larger in the hyperopes than in the myopes, and in both cases larger than the complete eye. We calculated a parameter (compensation factor) to describe the fraction of the corneal aberrations that were compensated by the lens for a particular eye. This parameter was given by $(RMS_{cornea} - RMS_{eye}) / RMS_{cornea}$.

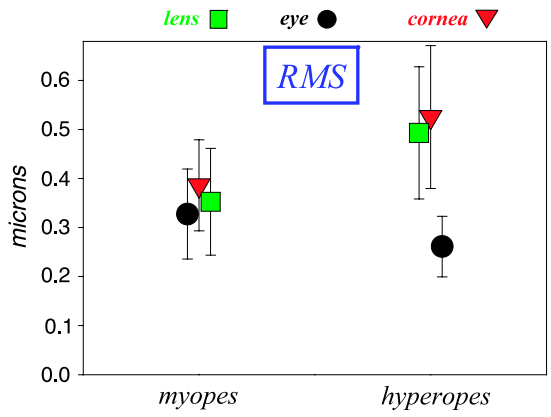

Figure 3. RMS in microns of the average aberrations for the lens (green squares), the eye (black circles), and the cornea (red triangles) in the myopic and hyperopic groups. Error bars indicate standard deviation for this and the following figures.

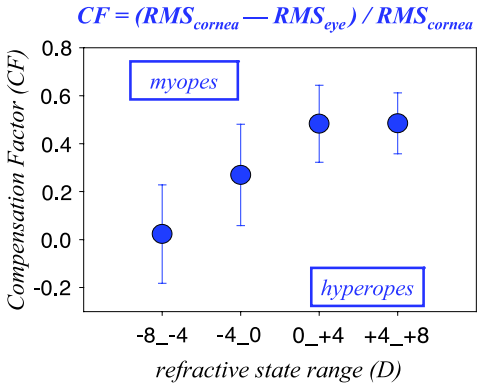

Figure 4. Compensation factor as a function of refractive error. The number of eyes included in the four refractive groups were 21, 37, 7, and 9, respectively (from myopic to hyperopic). The average age of the subjects in each group was 31.2, 28, 34.2, and 32.3 years old, respectively.

Positives values indicate compensation; small values around zero, a lack of compensation; and eventually negative values would note an addition of aberrations by the lens. Figure 4 presents this compensation factor averaged for four groups of subjects with different range of refractive errors, from high myopes (left) to hyperopes (right). Except for the high myopes, all the subjects presented some degree of compensation, although it is larger in the hyperopic eyes.

We further explored the behavior of specific aberration terms in each group of eyes. The average value of spherical aberration (Figure 5) was similar in both groups: it is positive for the cornea, negative for the lens and slightly positive for the complete eye. In most eyes, regardless of refractive error, spherical aberration was well compensated.

Figure 6 show the magnitude (absolute value) of trefoil, coma, and fourth-order aberration terms for the groups of myopic (Figure 6a) and hyperopic (Figure 6b) eyes. For the complete eye, these aberrations were found to be similar on

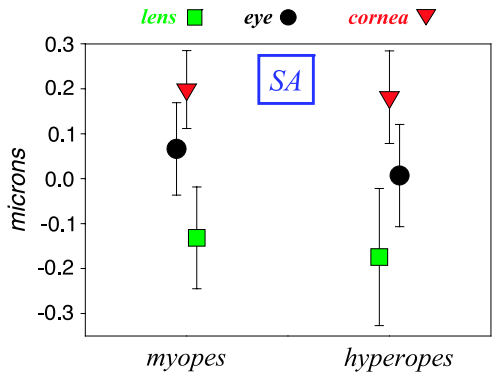

Figure 5. Average spherical aberration (SA) in microns for the lens (green squares), the eye (black circles), and the cornea (red triangles) in the myopic and hyperopic groups.

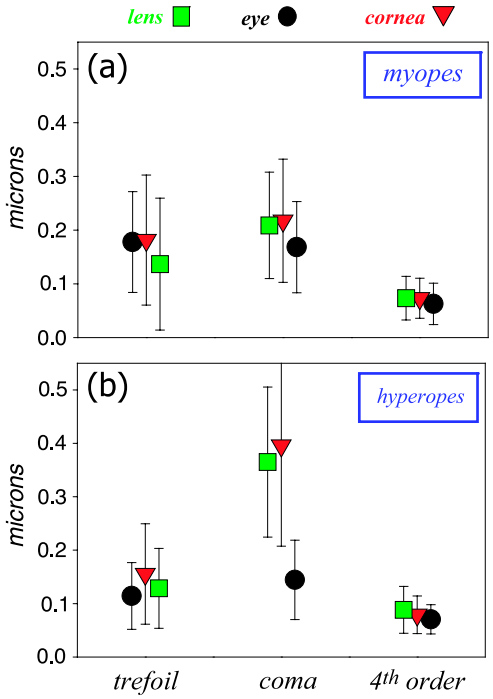

Figure 6. (a) Average magnitude of trefoil, coma, and fourth order aberration terms for the lens (green squares), the eye (black circles), and the cornea (red triangles) in the group of myopes. (b) Average magnitude of trefoil, coma, and fourth order aberration terms for the lens (green squares), the eye (black circles), and the cornea (red triangles) in the group of hyperopes.

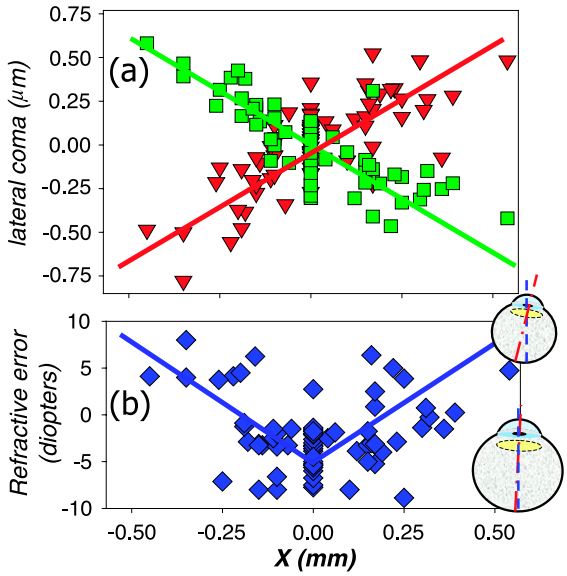

Figure 7. (a) Lateral coma in microns for the cornea (red triangles) and the lens (green squares) as a function of the value of pupil decentration in the horizontal direction (X) in millimeters. (b) Refractive error (in diopters) as a function of horizontal pupil decentration (X) in millimeters. On the left, it is represented a schematic representation of a hyperopic eye (shorter with larger kappa angle) and a myopic eye (longer with a smaller κ angle).

average in both groups. However, in the hyperopes, coma of both the cornea and the lens is nearly double that in the myopic group, indicating a more significant compensation of coma in hyperopes. In particular, lateral coma presents the most remarkable compensation.

Figure 7a shows, for all studied eyes, the amount of lateral coma for the cornea (red triangles) and the lens (green squares) as a function of pupil decentration in the horizontal direction (X). Those eyes with small values of pupil decentration present smaller values of coma in both the cornea and the lens. However, eyes with larger pupil decentration have a higher coma in both the cornea and the lens, although with opposite sign. This is the reason that coma in the complete eye remains within a normal range despite high values for both the cornea and the lens. On the other hand, those eyes with larger pupil decentration are usually shorter eyes, with a larger angle kappa. These are the normal geometrical features of hyperopic eyes (Le Grand & El Hage, 1980). On the contrary, smaller values of pupil decentration are commonly found in longer eyes that correspond with the myopic eyes. These eyes have lower values of coma in both ocular components a smaller overall compensation. Figure 7b shows the refractive error as a function of horizontal pupil decentration (X) for the same eyes as in Figure 7a.

Discussion

These results show how the components of the eye behave as an auto-compensating design producing similar overall optical quality in average for the different refractive groups, despite the large scale of possible structural variations. This is a remarkable example of robust design that supports a passive, simple geometrical model for the mechanism of compensation of ocular aberrations. In most subjects, both corneal and internal spherical aberrations are similar in magnitude but opposite in sign. Large values of corneal coma, caused by oblique incidence, occur in eyes with larger kappa angle, usually the hyperopic shorter eyes. The same condition, oblique incidence, generates coma with the opposite sign in the crystalline lens. Figure 8a schematically shows this situation in a model eye. Figure 8b represents the lateral coma for both the cornea and the lens as a function of the angle of incidence, calculated using ZEMAX ray-tracing software. This prediction should be compared with the actual measurements of coma of Figure 7a. The difference between the experimental data and this model can be understood as the contribution to coma due to the intrinsic shape of cornea and lens and the linear prediction by the model arises as a result of oblique incidence. This fact concerning coma was also previously suggested by Kelly et al. (2004). Their Figure 10 shows a similar prediction for coma using two different schematic eye models.

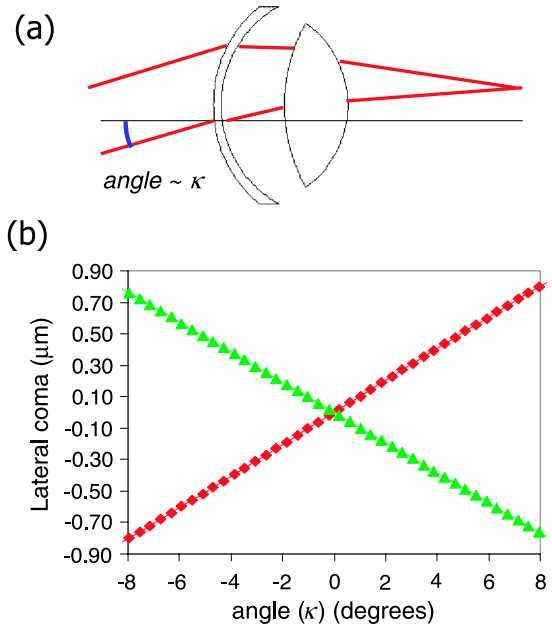

Figure 8. (a) Schematic diagram of a model eye with oblique incident (angle κ). (b) Lateral coma in microns for the cornea (red triangles) and the lens (green squares) as a function of the incident angle (κ), calculated in a model eye using a ray-tracing program.

It is interesting to note that the eye is a robust system simply to product a moderate image quality, but usually adequate to match the retinal mosaic resolution. If a more demanding image quality would be required, approaching diffraction limit, the situation would be different.

To further emphasize these findings, Figure 9 shows some examples of results in two typical eyes. Figure 9a shows the wave aberration maps for the complete eye, the cornea, and the lens in one eye with small κ angle, (and small X value), typically corresponding to a myopic eye. Spherical aberration is positive for the cornea and negative for the lens. The absolute magnitude is in general similar, although the corneal spherical aberration is slightly larger. Independent of refractive error, most young eyes displays this type of behavior concerning spherical aberration of the cornea and lens. This may be understood as a result of evolution working toward corneal and lenticular shapes that balance the spherical aberration of one another. Our results confirm this scenario, similar to one previously proposed (Kelly et al., 2004). As mentioned previously, this situation changes during the process of normal aging (Artal et al., 2002). The spherical aberration of the cornea remains relatively stable (Guirao et al., 2000), but the lens changes becoming more positive and thereby removing the compensatory effect. The induced lateral coma of the cornea and the lens is linearly dependent on the κ angle, but with opposite signs (Figure 8b).

Figure 9b shows wavefront aberration maps in an example of a real hyperopic eye. The relative decentering

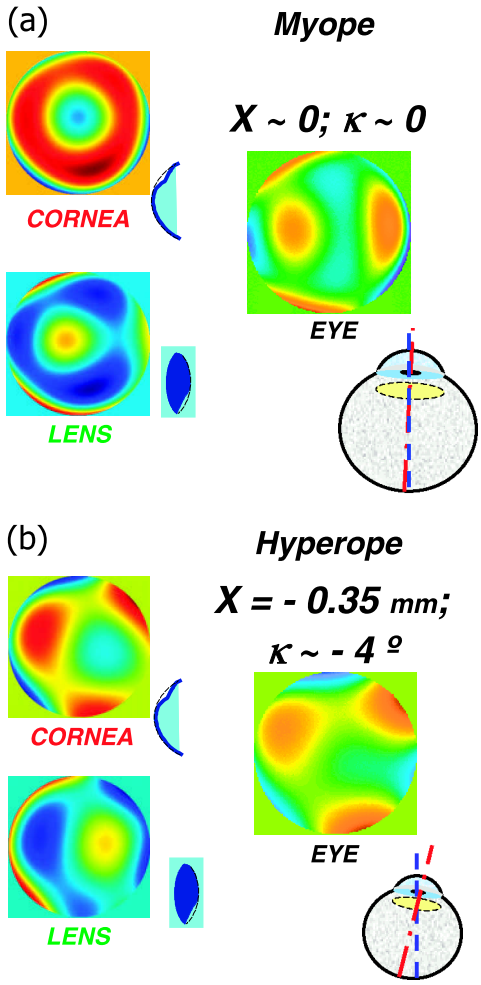

Figure 9. (a) Wave aberration maps for the cornea, lens and complete eye in a myopic eye with a small value of angle κ. (b) Wave aberration maps for the cornea, lens and complete eye in a hyperopic eye with a large value of angle κ.

of the pupil and the κ angle are negative so that the lateral coma induced in both the cornea and the lens have opposite signs and approximately cancel each other out. It is important to note that this is a simplified model. The actual situation is more complicated: Both the cornea and the lens have per se some amounts of coma even for normally incident light, and because of this the compensation is only partial. In addition, the lens itself is tilted and decentered inducing other higher order aberration beyond those described herein. However, these two effects, compensation of lateral coma and spherical aberration, are quite stable and possibly the result of a robust design of the eye's optics.

Conclusions

We explored the nature of the mechanism of the compensation of the aberrations within the human eye by analyzing eyes with different refractive errors. If defocus

and astigmatism are excluded, eyes with very different geometrical features have similar optical performance. This is a remarkable example of an auto-compensating mechanism for the optics of the eye. These results may indicate a passive, geometry-driven mechanism for aberration compensation in the normal young eye leading to a simple but at the same time extremely robust layout of the optical components in the eye. It must be pointed out that these results are not completely excluding the option of some active process (or visually guided) of compensation. It can be possible that a combination of both processes actually occurs.

Acknowledgments

This research was supported in part by grants from the Spanish *Ministerio de Educación y Ciencia* (BFM2001-0391 & FIS2004-2153). The authors thank M. Redondo for performing the ophthalmic testing of subjects participating in this study. We also thank S. Burns, D.G. Green, S. Klyce, P. Piers, P. Prieto, F. Schaeffel, J. Santamaría, and D.R. Williams for revising the manuscript or ample discussions with the authors. Presented in part at the annual meeting of the Association for Research in Vision and Ophthalmology, Fort Lauderdale, Florida, 2004 (Benito & Artal, 2004).

Commercial relationships: none.
Corresponding author: Pablo Artal.
Email: pablo@um.es.
Address: Laboratorio de Optica, Departamento de Fisica, Universidad de Murcia, Campus de Espinardo (Edificio C), 30071 Murcia, Spain.

References

Artal, P. (2004). Combining corneal and ocular wave-aberrations. In *Wavefront customized visual correction* (chap. 37, pp. 311–317). Thorofare, NJ: Slack.

Artal, P., Berrio, E., Guirao, A., & Piers, P. (2002). Contribution of the cornea and internal surfaces to the change of ocular aberrations with age. *Journal of the Optical Society of America. A, 19,* 137–143. [PubMed]

Artal, P., & Guirao, A. (1998). Contributions of the cornea and the lens to the aberrations of the human eye. *Optics Letters, 23,* 1713–1715.

Artal, P., Guirao, A., Berrio, E., & Williams, D. R. (2001). Compensation of corneal aberrations by internal optics in the human eye. *Journal of Vision, 1*(1), 1–8, http://journalofvision.org/1/1/1/, doi:10.1167/1.1.1. [PubMed] [Article]

Artal, P., & Navarro, R. (1994). Monochromatic modulation transfer function of the human eye for different pupil diameters: An analytical expression. *Journal of the Optical Society of America. A, 11,* 246–249. [PubMed]

Benito, A., & Artal, P. (2004). Compensation of corneal aberrations by the internal optics is better in hyperopic eyes [Abstract]. *Investigative Ophthalmology and Visual Science, 45,* 1076.

Cheng, X., Bradley, A., Hong, X., & Thibos, L. (2003). Relationship between refractive error and monochromatic aberrations of the eye. *Optometry and Vision Science, 80,* 43–49. [PubMed]

Fernández, E. J., Iglesias, I., & Artal, P. (2001). Closed-loop adaptive optics in the human eye. *Optics Letters, 26,* 746–748.

Glasser, A., & Campbell, M. C. W. (1998). Presbyopia and the optical changes in the human crystalline lens with age. *Vision Research, 38,* 209–229. [PubMed]

Grosvenor, T., & Goss, D. A. (1999). *Clinical management of myopia*. Boston: Butterworth-Heinemann.

Guirao, A., & Artal, P. (2000). Corneal wave aberration from videokeratography: Accuracy and limitations of the procedure. *Journal of the Optical Society of America. A, 17,* 955–965. [PubMed]

Guirao, A., Redondo, M., & Artal, P. (2000). Optical aberrations of the human cornea as a function of age. *Journal of the Optical Society of America. A, 17,* 1697–1702. [PubMed]

Hofer, H., Artal, P., Singer, B., Aragón, J. L., & Williams, D. R. (2001). Dynamics of the eye's wave aberration. *Journal of the Optical Society of America. A, 18,* 497–506. [PubMed]

Howland, B., & Howland, H. C. (1976). Subjective measurement of high-order aberrations of the eye. *Science, 193,* 580–582. [PubMed]

Kelly, J. E., Mihashi, T., & Howland, H. C. (2004). Compensation of corneal horizontal/vertical astigmatism, lateral coma, and spherical aberration by internal optics of the eye. *Journal of Vision, 4*(4), 262–271, http://journalofvision.org/4/4/2/, doi:10.1167/4.4.2. [PubMed] [Article]

Le Grand, Y., & El Hage, S. G. (1980). *Physiological optics*. Berlin: Springer-Verlag.

Liang, J., Grimm, B., Goelz, S., & Bille, J. F. (1994). Objective measurement of wave abberations of the human eye with the use of a Hartmann–Shack wavefront sensor. *Journal of the Optical Society of America. A, 11,* 1949–1957. [PubMed]

Liang, J., & Williams, D. R. (1997). Aberrations and retinal image quality of the normal human eye. *Journal of the Optical Society of America. A, 14,* 2873–2883. [PubMed]

Noll, R. J. (1976). Zernike polynomials and atmospheric turbulence. *Journal of the Optical Society of America. A, 66,* 207–211.

Prieto, P. M., Vargas-Martín, F., Goelz, S., & Artal, P. (2000). Analysis of the performance of the Hartmann–Shack sensor in the human eye. *Journal of the Optical Society of America. A, 17,* 1388–1398. [PubMed]

Schaeffel, F., & Diether, S. (1999). The growing eye: An autofocus system that works on very poor images. *Vision Research, 39,* 1585–1589. [PubMed]